Ultrasonics 91 (2019) 129–133

Contents lists available at ScienceDirect

Ultrasonics

journal homepage: www.elsevier.com/locate/ultras

Short communication

Modulating acoustic Fano resonance of self-collimated sound beams in two dimensional sonic crystals

Ting Zhang[a,b], ShuXiang Gao[a], Ying Cheng[a,c,*], XiaoJun Liu[a,c,*]

[a] Key Laboratory of Modern Acoustics, Department of Physics and Collaborative Innovation Center of Advanced Microstructures, Nanjing University, Nanjing 210093, China
[b] School of Electronic & Information Engineering, Nanjing University of Information Science & Technology, Nanjing 210044, China
[c] State Key Laboratory of Acoustics, Chinese Academy of Sciences, Beijing 100190, China

ARTICLE INFO

Keywords:
Acoustic Fano resonance
Self-collimating effect
Sonic crystals

ABSTRACT

Controlling the lineshape of Fano resonance has great potential applications. Here we propose a type of acoustic Fano resonator, which is composed of a multi-layer zigzag line defects (ZLDs) sandwiched by double-layer zigzag steel rods in two-dimensional sonic crystals (SCs). We have theoretically and experimentally observed the asymmetric Fano resonances caused by the interference between the resonant and propagating self-collimated acoustic waves. It is demonstrated that the resonance dip frequency and Fano profile can be modulated by adjusting the structure parameters of the SC-based resonator. Our finding provides an efficient approach to manipulate sound propagation for future acoustic devices.

1. Introduction

The Fano resonance is caused by the destructive and constructive interference between a discrete energy state (the resonant process) and a continuum energy state (the background process). Its asymmetric lineshape and ultra-narrow linewidth are distinctively different from that of the conventional symmetric Lorentzian-like resonance [1]. Over the recent past, optical Fano resonance has attracted much attention due to numerous applications such as switching [2,3], lasing [4], biosensing [5–7], and slow-light technologies [9,10], which require comparable high frequency sensitivity or strong resonant and radiated mode. The system that supports Fano-like resonance usually requires complex unit cell with symmetry-breaking structures such as dipole quadrupole coupled metamaterials or metasurfaces [4,5], waveguide-Plasmon coupled systems [7], asymmetric split ring resonators [8] and so on. However, very few efforts [11–14] has been devoted to the modulation of the Fano resonance lineshape, e.g. linewidth, resonance frequency, spectral contrast, which in fact largely determines the overall performance of the Fano-resonance-based devices, such as the detection limit of biosensor. By selectively altering the particle shape of either subgroup of plasmonic nanoclusters, Rahmani et al realized a lineshape tunable and designable Fano resonance, and employed a deconstruction method to explain the superposition of a subradiant and a superradiant state of the system [12]. Recently, Li et al and Deng et al proposed independently of semi-independently tunable Fano resonance in two kinds of optical systems by changing the parameters of the resonance structures [13].

Fano resonance is a general phenomenon, which is ubiquitous in many areas of physics and engineering. Note that the *Q*-factor of Fano resonance is much higher than that of the Lorentzian resonance, which directly determine the sensitivity of the sensor [5,6]. In addition, due to the distinct physical properties such as wavelength and propagation medium, the manipulation of acoustic waves is of more importance than optic waves under certain circumstances. Specially, the optic signals exhibit high attenuation and short transmission distance in underwater and medical applications. Thus, the Fano resonance of acoustic waves has attracted increasing attention recently [15–22]. Excepting for the analytically investigation of the Fano resonance in one- or two-dimensional waveguides with obstacles or localized resonator, a series of acoustic devices based on Fano resonance have been proposed and demonstrated. Wang et al [18] and Amin et al [19] both realized acoustically induced transparency (AIT) devices based on Fano resonance by coupling a small concentric shell (pipe) with a bigger one. Yang et al realized a broadband acoustic superlens using Helmholtz-resonator-based metamaterials, and point out that the corresponding mechanism is the Fano resonance rather than the conventional Fabry-Pérot resonance [20]. Oudich et al [21,22] investigated the Fano resonance of acoustic surface waves in phononic crystals based on pillars

* Corresponding authors at: Key Laboratory of Modern Acoustics, Department of Physics and Collaborative Innovation Center of Advanced Microstructures, Nanjing University, Nanjing 210093, China.
E-mail addresses: chengying@nju.edu.cn (Y. Cheng), liuxiaojun@nju.edu.cn (X. Liu).

https://doi.org/10.1016/j.ultras.2018.08.001
Received 25 April 2018; Received in revised form 11 June 2018; Accepted 3 August 2018
Available online 04 August 2018
0041-624X/

distributed on the substrate surface, which presents novel approach to accurate surface acoustic wave control for sensing applications. However, most of acoustic Fano resonances were results of interference of two near states, i.e., one with a high Q-factor and the other with a low Q-factor. Moreover, the Fano resonances have similar lineshape because the energy ratio between the two states cannot be arbitrarily adjusted. Thus, manipulating both the discrete and the continuum modes in acoustic Fano resonances is remained as a significant challenge.

On the other hand, artificial sonic crystals (SCs) and metamaterials have been widely investigated due to their plenty of non-natural occurring properties, such as negative refraction, near-zero index, extraordinary transmission, self-collimation and so on [23–27]. The self-collimation effect provides an effective approach to inhibit the propagating diffraction of sound waves in two-dimensional (2D) SCs. The self-collimation phenomenon of acoustic beam in a SC has attracted considerable attention due to the resulting wave-guiding properties such as diffractionless propagation along a definite direction and easy crossing without cross talk. Based on the interference of the self-collimated sound waves, a series of acoustic devices, such as acoustic switches, acoustic sensing and acoustic logic gates have been proposed and demonstrated [26,28,29]. The realization of the Fano resonance of self-collimated beams in a SC is a high-potential research field because it could increase the possibility of application of self-collimated beams. Here, we proposed a SC-based structure that can supports evident asymmetric Fano resonance of self-collimated sound beams. Since the self-collimation effect occurs due to the complex dispersion properties of the propagation modes instead of bandgap in a SC, the resonant cavity should locate on the propagating path of the self-collimated beams. The Fano resonator is composed of zigzag line defects (ZLDs) sandwiched by two columns of zigzag steel rods. Due to the interference between the radiated sound beams from the resonator and the directly propagated self-collimated sound beams, the transmission spectrum shows an evident asymmetric Fano lineshape. Moreover, the dip position and the lineshape (usually described by the Fano factor q) can be continuously and semi-independently adjusted in a wide frequency range by adjusting the structure parameters, such as the radii of the ZLD rods and the steel rods of the resonator in 2D SCs. The Fano resonance of the self-collimated sound beams with high quality factor Q and designable lineshape may be used in integrated acoustic devices, such as filters, sensors and acoustic switches.

2. Simulation and experiment

In order to investigate the Fano resonance, a nearly flat background mode could be valuable for understanding and controlling the performance of the Fano resonance. Here we consider the self-collimation effect of sound beams in 2D SCs as the background mode. The simulations are performed by the Acoustic-Structure Interaction in COMSOL Multiphysics, which characterize the effect of acoustic-structure interaction by including the shear modulus of the solid materials. A square lattice of 2D SCs composed of epoxy resin rods immersed in water with a filling ratio of 0.196 is constructed. The density and acoustic longitudinal speed are $\rho_w = 998\,kg/m^3$ and $c_w = 1483\,m/s$ for water; the density, Young's modulus and Poisson's ratio are $\rho_e = 1180\,kg/m^3$, $E_e = 5.35\,GPa$ and $\sigma_e = 0.35$ for epoxy; $\rho_s = 7800\,kg/m^3$, $E_s = 20.6\,GPa$ and $\sigma_s = 0.28$ for steel, respectively. The unit lattice of the employed SC and the equifrequency contours (EFCs) corresponding to the first band in the first Brillouin zone are shown in Fig. 1(a). For convenience, the frequency is normalized by c_w/a. Here, a is the lattice constant. As shown by the arrow in Fig. 1(a), the EFC is flat and normal to the Γ-M direction at the normalized frequency $f = 0.58$. Thus, the acoustic waves at $f = 0.58$ should propagate along the Γ-M direction without diffraction. The insert of Fig. 1(b) shows the sound field distribution of the propagating self-collimated beam at $f = 0.58$ in a SC with a size $20\sqrt{2}a \times 13\sqrt{2}a$. Note that the incident monochromatic acoustic beam propagates along the Γ-M direction without beam spreading in the SC and its flat wavefront is perpendicular to the propagation direction. We also investigate the transmittance of sound beams from $f = 0.553$ to 0.58 and find that more than 96% of the incident power is transmitted through the SC, which is suitable as a background mode, as shown in Fig. 1(b).

Fig. 2(a) shows the schematic of the Fano resonator which is composed of a ZLD sandwiched by double-layer steel rods in a $14\sqrt{2}a \times 20\sqrt{2}a$ 2D SC block. In order to generate a strong trapped mode, we set the radius of steel rods larger than the rods in the SC while the radius of the line defect rods smaller than the rods in the SC. The propagation direction and effective speed of the acoustic beams in the SC are determined by the gradient of the band structure [30]: $v_g = \nabla_k f(k)$. Here the radius of the surrounding resin rods is $r_0 = 0.25a$, while the radii of the ZLDs rods and steel rods are $r_d < r_0$ and $r_s > r_0$, respectively. The length and width of the resonator are $14\sqrt{2}a$ in the y-direction and $4\sqrt{2}a$ in the x-direction, respectively. The self-collimated sound beams can be strongly reflected by the zigzag shaped boundary due to the index difference and wavefront mismatch. The incident self-collimated beam broken by one side of the resonator should be reconstructed by another one. When the self-collimated sound beam propagates into the resonator, a part of the incident beam should be trapped by the resonator and reradiated again. Consequently, the interference between the radiated sound beam S_r (trapped mode) and the self-collimated beam S_t which passes through the resonator (background mode) gives rise to the Fano resonance, as shown in Fig. 2(a).

The classic Fano lineshape can be described as the following [11]

$$T(f) = A\,\frac{[q + 2(f-f_0)/\Delta]^2}{1 + [2(f-f_0)/\Delta]^2} \tag{1}$$

Here A is a constant, q is the Fano factor, f_0 is the resonant frequency and Δ is the resonance bandwidth. In order to demonstrate the Fano resonance, the transmission spectra in the self-collimation frequency range of the proposed resonator are investigated. Here we first keep the steel rods radius $r_s = 0.35a$ and inspect the transmission spectra with varying ZLD radius r_d. Fig. 2(b) shows the transmission spectra of the self-collimated beams passing through the ZLDs resonator. The rod radii are $r_d = 0.02a$, $0.08a$ and $0.12a$, respectively. From Fig. 2(b), the evident asymmetric Fano lineshape is observed in the transmission spectra, and the dip position moves from $f = 0.559$ to 0.595 as the radius of the ZLD rods increases. The blue shift of the dip position and the observable bandwidth shrinking of the transmission spectra are caused by the increase of effective sound speed as the radius of the ZLD rods increases [30]. It is noticed that as r_d is closer to r_0, the resonance dip becomes shallower, indicating that the resonant mode becomes weaker as r_d increases. We further depict the sound field distributions of the resonator with $r_d = 0.02a$ at $f = 0.559$ [see Fig. 2(c)] and 0.563 [see Fig. 2(d)]. As shown in Fig. 2(c) and (d), the self-collimated sound beams at $f = 0.559$ barely transmits through the resonator due to the destructive interference between the trapped mode and the background mode, while most of (~91%) the self-collimated beams at $f = 0.563$ propagates through the resonator due to the constructive interference.

To verify above conceptual design and simulation results, we have achieved the Fano resonance in experiments. The measurement set-up and the prototype are shown in Fig. 3(a) and (b), respectively. In order to eliminate the influence of the reflected waves, the tank was covered with sound-absorbing wedges. One unfocused transducers centered at a frequency of 0.1 MHz were employed as the sound source, and one unfocused transducers centered at a frequency of 0.1 MHz as the receiver. The acoustic signal launched by the transducer through the SC sample was detected by the detective transducer. The acquired signals were sent to a low noise preamplifier, and then processed by the LabVIEW application. Time domain data was finally analyzed after averaging 30 measurements. In the experiment, we detected the transmitted acoustic signals passed through two prototypes with different parameters, e.g. $r_s = 0.35a$, $r_d = 0$; $r_s = 0.35a$, $r_d = 0.1a$. For convenience, we only measured the point sound pressure from the output side but not

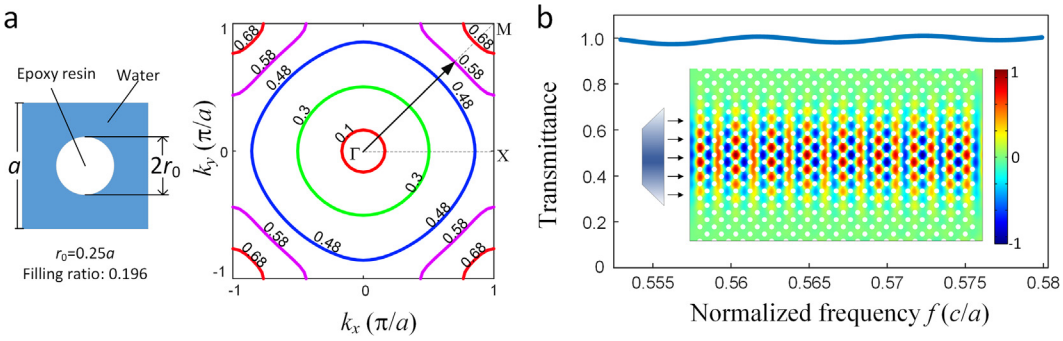

Fig. 1. Acoustic self-collimation effect: (a) The unit lattice of the employed 2D SC and the EFCs of the first band structure in the first Brillouin zone. The EFC at $f = 0.58$ is nearly flat and normal to the Γ-M direction. (b) The simulated power transmittance of the self-collimated sound beams in the frequency ranging from 0.553 to 0.58. Insert shows the sound field distribution of a propagating self-collimated beam at $f = 0.58$.

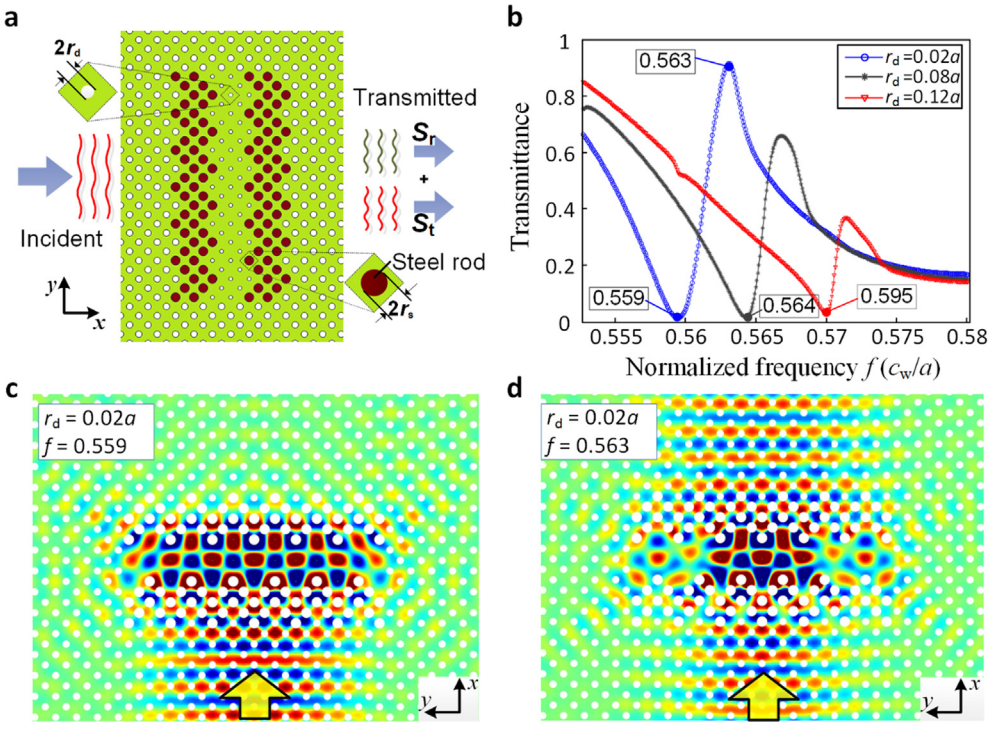

Fig. 2. Schematic of the Fano resonator and the simulation results for the two-layer ZLD resonator: (a) Schematic view of the proposed Fano resonator, which is composed of a two-layer ZLD rods of a radius r_d sandwiched by two columns of zigzag steel rods of a radius r_s. Fano resonance occurs due to the interference between the radiated sound beam S_r and the self-collimated beam S_t that directly passes through the resonator without resonance. (b) Power transmission spectra of the two-layer ZLD resonator at $r_d = 0.02a$, $0.08a$ and $0.12a$. Sound field distributions of the self-collimated beams at (c) $f = 0.559$ and (d) $f = 0.563$ when $r_d = 0.02a$.

the transmission coefficient.

For each frequency, we made 30 measurements, and the finally analyzed transmission spectra together with the simulation results are shown in Fig. 4: (a) $r_s = 0.35a$, $r_d = 0$ and (b) $r_s = 0.35a$, $r_d = 0.1a$. The evident Fano lineshapes are found for the experiment and simulation transmission spectra, as shown in Fig. 4. In Fig. 4(a), the dip and the peak positions of the two transmission spectra are coincide with each other, but the amplitudes show some bias at the frequencies away from the resonant frequency. In Fig. 4(b), the measured sound pressure amplitude is relatively lower than that of the simulation result, and the bandwidth is slightly broader than that of the simulation spectrum. We further calculated the quality factor $Q = \frac{f_0}{(f_{peak} - f_{dip})}$ for the transmission spectra, where f_{peak} is the peak frequency, f_{dip} is the dip frequency, f_0 is the center frequency. The Q values are both 153 for experiment and simulation in Fig. 4(a), while Q is 188 for experiment but 249 for simulation in Fig. 4(b). These deviations may be caused by the manufacturing deviation of the prototype, inevitable bias during the experiment, and the sound speed of the water. Thus, we have theoretically and experimentally achieved the Fano resonance of the self-collimated sound beams in two dimensional sonic crystals.

3. Discussion

The Fano factor q is the most important factor to identify the Fano lineshape. The value of the Fano factor q is correlated to the energy ratio between the trapped mode and the background mode. Thus, it is reasonable to expect that the energy of background mode can be controlled by adjusting the radius of the steel rods r_s.

Fig. 5(a) shows the evolution of the transmission spectra with r_s. Here, r_s varies from $0.31a$ to $0.38a$ while $r_d = 0$. It is found that the energy of the propagation mode gradually decreases with the increase of r_s, while the resonance lineshape shows a dramatically evolution from a reversed Lorentzian lineshape to an evident asymmetric Fano lineshape, as shown in Fig. 5(a). The Fano factors q of the curves in Fig. 5(a) can be achieved by fitting them to the Eq. (1). The results show that the Fano factor q increases from 0.1 to 6.7 as r_s varying from $0.31a$ to $0.38a$, which is coordinate with the evolution of the lineshape. A blue shift of the resonance position is also observed in Fig. 5(a), which can be ascribed to the reduction of the resonator's width and the increase of r_s. In Fig. 5(b), the evolution of the transmission spectrum with the radius of the ZLD rods r_d is further investigated. Here, r_d varies from $0.02a$ to $0.16a$ while $r_s = 0.35a$. It is found that the position of the

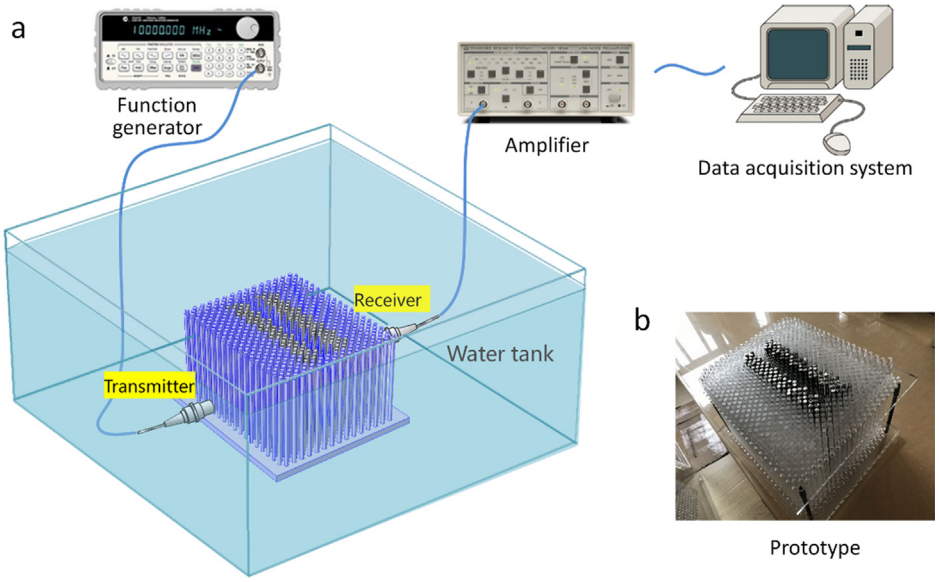

Fig. 3. Experimental demonstration of the Fano resonance: (a) Schematic of the experimental setup. (b) The photograph of the prototype of the Fano resonator fabricated by using epoxy resin rods.

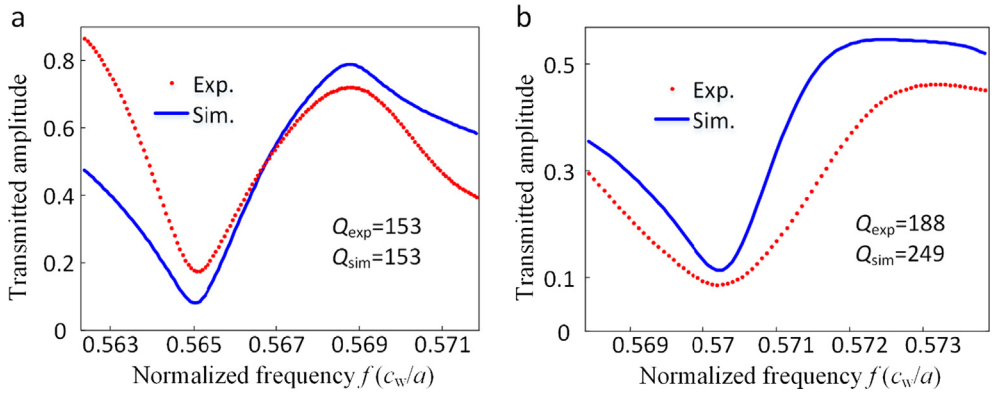

Fig. 4. The experimental and simulation transmission amplitudes of the acoustic beams with (a) $r_s = 0.35a$, $r_d = 0$ and (b) $r_s = 0.35a$, $r_d = 0.1a$.

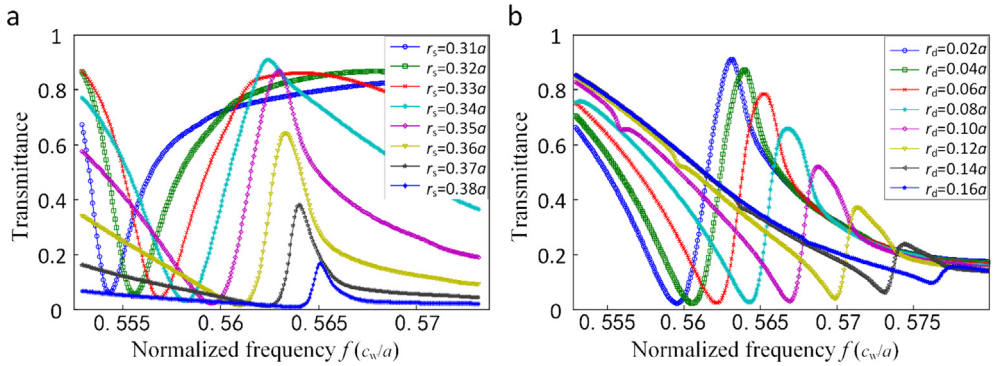

Fig. 5. The evolution of the power transmission spectra with respect to the radii of the steel rods r_s and the ZLD rods r_d: (a) The evolution of the power transmission spectrum at $r_d = 0$ with r_s varying from $0.31a$ to $0.38a$. (b) The evolution of the power transmission spectrum at $r_s = 0.35a$ with r_d varying from $0.02a$ to $0.16a$.

trapped mode shows a blue shift with the increase of r_d, but the background mode is almost unchanged, resulting that the lineshape maintains the asymmetric Fano resonance profile with a Fano factor $q \approx 1$. We also observe that the resonant mode becomes weaker as r_d increases, which is consistent with that in Fig. 2. Therefore, the lineshape of the transmission spectrum profile can be changed by adjusting the radius of the steel rods r_s. And then the Fano resonant frequency can be adjusted by altering the radius of the ZLDs of the resonator. These behaviors provide us a convenient approach to control both the trapped and background modes independently or simultaneously. Therefore, by properly choosing the structure parameters of the resonator, the transmission spectra of the Fano resonance can be arbitrarily designed.

4. Conclusion

In summary, by introducing a trapped mode into propagation mode,

the asymmetric Fano resonance of self-collimated acoustic beams can be achieved in 2D SCs. The Fano resonator is composed of a two-layer of ZLDs sandwiched by two columns of zigzag steel rods. We find that the asymmetric of the Fano lineshape can be continuously tuned by the radius of the steel rods, while the resonance frequency can be adjusted by the radius of the ZLD rods. The designable Fano resonance of self-collimated sound beams in 2D SCs could provide an efficient approach to manipulate sound propagation, which may lead to convenient and flexible applications such as acoustic sensing and switching.

Acknowledgements

This work was supported by the National Basic Research Program of China (Grant No. 2017YFA0303702), NSFC (Grant Nos. 11674172, 11574148 and 11474162), and the Fundamental Research Funds for the Central Universities (Grant Nos. 020414380001 and 020414380053).

References

[1] U. Fano, Phys. Rev. 124 (1961) 1866–1878.
[2] K. Nozaki, A. Shinya, S. Matsuo, T. Sato, E. Kuramochi, M. Notomi, Opt. Express 21 (2013) 11877–11888.
[3] M. Heuck, P. Kristensen, T.Y. Elesin, J. Mørk, Opt. Lett. 38 (2013) 2466–2468.
[4] Y.K. Srivastava, M. Manjappa, L. Cong, W. Cao, I. Al-Naib, W. Zhang, R. Singh, Adv. Opt. Mater. 4 (2015) 457–463.
[5] R. Singh, W. Cao, I. Al-Naib, L.Q. Cong, W. Withayachumnankul, W.L. Zhang, Appl. Phys. Lett. 105 (2014) 171101.
[6] S. Amoudache, R. Moiseyenko, Y. Pennec, B.D. Rouhani, A. Khater, R. Lucklum, R. Tigrine, J. Appl. Phys. 119 (2016) 114502.
[7] B. Yun, G. Hu, R. Zhang, Y. Cui, J. Opt. 18 (2016) 055002.
[8] C. Wu, A.B. Khanikaev, R. Adato, N. Arju, A.A. Yanik, H. Altug, G. Shvets, Nat. Mater. 11 (2012) 69–75.
[9] B. Luk'yanchuk, N.I. Zheludev, S.A. Maier, N.J. Halas, P. Nordlander, H. Giessen, C.T. Chong, Nat. Mater. 9 (2010) 707–715.
[10] G. Lai, R. Liang, Y. Zhang, Z. Bian, L. Yi, G. Zhan, R. Zhao, Opt. Express 23 (2015) 6554.
[11] S. Lee, J. Park, C. Kee, Opt. Express 22 (2014) 28954.
[12] M. Rahmani, D.Y. Lei, V. Gianini, B. Lukiyanchuk, M. Ranjbar, T.Y.F. Liew, M. Hong, S.A. Maier, Nano Lett. 12 (2012) 2101–2106.
[13] S. Li, Y. Zhang, X. Song, Y. Wang, L. Yu, Opt. Express 24 (2016) 15351.
[14] Z.L. Deng, N. Yogesh, X.D. Chen, W.J. Chen, J.W. Dong, Z. Ouyang, G.P. Wang, Sci. Rep. 5 (2015) 18461.
[15] E.H.E. Boudouti, T. Mrabti, H. Al-Wahsh, B. Djafari-Rouhani, A. Akjouj, L. Dobrzynski, J. Phys. Condens. Metter 20 (2008) 255212.
[16] D. Nardi, M. Travagliati, M.E. Siemens, Q. Li, M.M. Murnane, H.C. Kapteyn, G. Ferrini, F. Parmigiani, F. Banfi, Nano Lett. 11 (2011) 4126–4133.
[17] L. Qi, G. Yu, X. Wang, G. Wang, N. Wang, J. Appl. Phys. 116 (2014) 234506.
[18] M. Amin, A. Elayouch, M. Farhat, M. Addouche, A. Khelif, H. Bağcı, J. Appl. Phys. 118 (2015) 164901.
[19] G. Wang, L. Jin, P. Li, Z. Xu, Appl. Phys. Lett. 109 (2016) 073503.
[20] X.S. Yang, J. Yin, G.K. Yu, L.H. Peng, N. Wang, Appl. Phys. Lett. 107 (2015) 193505.
[21] M. Oudich, B. Djafari-Rouhani, B. Bonello, Y. Pennec, F. Sarry, Crystals 7 (2017) 372.
[22] M. Oudich, B. Djafari-Rouhani, B. Bonello, Y. Pennec, S. Hemaidia, F. Sarry, D. Beyssen, Phys. Rev. Appl. 9 (2018) 034013.
[23] Z.X. Liang, J. Li, Phys. Rev. Lett. 108 (2012) 114301.
[24] Y. Cheng, C. Zhou, B.G. Yuan, D.J. Wu, Q. Wei, X.J. Liu, Nat. Mater. 14 (2015) 1013–1019.
[25] J.Y. Lu, C.Y. Qiu, M.Z. Ke, Z.Y. Liu, Phys. Rev. Lett. 116 (2016) 093901.
[26] T. Zhang, Y. Cheng, J.Z. Guo, J.Y. Xu, X.J. Liu, Appl. Phys. Lett. 106 (2015) 113503.
[27] Z.W. Zhang, Q. Wei, Y. Cheng, T. Zhang, D.J. Wu, X.J. Liu, Phys. Rev. Lett. 118 (2017) 084303.
[28] S. Alagoz, B.B. Alagoz, J. Acoust. Soc. Am. 133 (2013) 485–490.
[29] O.A. Kaya, A. Cicek, A. Salman, B. Ulug, Sensor Actuat. B-Chem. 203 (2014) 197–203.
[30] S.S. Lin, T.J. Huang, Phys. Rev. B 79 (2009) 094302.